Anomalous water optical absorption: Large-scale *first-principles* simulations

W.G. Schmidt[1,3], S. Blankenburg[1], S. Wippermann[1], A. Hermann[2], P.H. Hahn[3], M. Preuss[3], K. Seino[3], and F. Bechstedt[3]

[1]Theoretische Physik, Universität Paderborn, 33095 Paderborn, Germany
[2]Institute of Fundamental Sciences, Massey University, Auckland, New Zealand
[3]Institut für Festköpertheorie und -optik, Friedrich-Schiller-Universität Jena, Germany

Summary. The optical spectrum of water is not well-understood. For example, the main absorption peak shifts *upwards* by 1.3 eV upon condensation of gas-phase water monomers, which is contrary to the behaviour expected from aggregation-induced broadening of molecular levels. We investigate theoretically the effects of electron-electron and electron-hole correlation, finding that condensation leads to delocalisation of the exciton onto nearby hydrogen-bonded molecules. This reduces its binding energy and has a dramatic impact on the line shape. The calculated spectrum is in excellent agreement with experiment.

1 Introduction

Despite the apparent simplicity of the water molecule, the hydrogen bonds between aggregated water molecules cause many peculiarities that still elude understanding. The thorough, microscopic understanding of water in its various phases is not only of fundamental interest, but forms the prerequisite for any serious attempt to address the many chemical, biological and technological processes related to it. Here we address the water optical absorption, which is not well-understood, despite decades of effort. The spectra of amorphous, hexagonal as well as cubic ice are dominated by a very pronounced first absorption peak at about 8.7 eV [1, 2]. The absorption spectrum of the liquid shows a similar structure [3, 4]. In the case of cubic ice, the first absorption peak was attributed to the calculated density of states [5]. However, the universal occurrence of the 8.7 eV peak in a variety of water phases suggests its molecular origin, as opposed to being due to specific transitions between electronic states arising from a crystalline structure with a particular symmetry. However, the lowest-lying excitation of the H_2O molecule occurs at 7.4 eV [6]. Intermolecular interactions are expected to induce a significant broadening of the energy levels relative to the isolated molecule. This should lead to a decrease of the transition energies relative to the molecular values [7, 8, 9]. Numerical studies of the optical properties of ice [10] based on the local density approximation, *i.e.*, neglecting many-body effects beyond a mean-field description, indeed find the absorption onset at just below 6 eV.

The blueshift observed experimentally upon condensation of water molecules has been alternatively attributed to excitons of *molecular* origin [8, 9] or to solvation and Rydbergisation effects (destabilisation of highly excited states in condensed phases by interactions with nearby molecules) [11]. However, accurate description of optical spectra requires inclusion of many-body correlation effects from *first principles*, which is a difficult and computationally expensive task for complex disordered systems.

We exploit the recent progress in accurate modelling of optical properties using the many-body Green's function approach [12] to explain and quantitatively account for the peculiar absorption properties of solid water [13] and single water monomers [14]. The results highlight the major role played by nearby hydrogen-bonded water molecules in affecting the spacial extent and the energetics of the exciton dominating the main absorption peak. It is clear that the exciton state "sees" nearby molecules due to its spacial extent and will be affected by changes in the first and even the second coordination shell.

Naturally occurring hexagonal ice (ice-Ih) is chosen as a model system. The spectra of cubic and amorphous ice, however, are very similar. We proceed in three steps: (i) We use density-functional theory in generalized gradient approximation (DFT-GGA) to obtain the structurally relaxed ground state configuration of ice-Ih and the Kohn-Sham eigenvalues and eigenfunctions that enter the single- and two-particle Green's functions, (ii) the electronic quasiparticle spectrum is obtained within the GW approximation (GWA) [15] to the exchange-correlation self-energy, and (iii) the Bethe-Salpeter equation (BSE) is solved for coupled electron-hole excitations [16, 17, 18], thereby accounting for the screened electron-hole attraction and the unscreened electron-hole exchange [19, 20, 21].

The oxygen atoms in the ice-Ih structure lie on a hexagonal wurtzite lattice. Hydrogen atoms occupy the sites between neighbouring oxygens in a disordered fashion but subject to the ice rules, *i.e.*, each oxygen is covalently bonded to two hydrogen atoms with the constraint that only one H atom can lie between two neighboring O atoms. We model the proton disorder within a periodically repeated supercell consisting of 16 molecules [22].

2 Computational Method

We start from *first-principles* pseudopotential calculations within the DFT-GGA [23]. The mean-field effects of exchange and correlation in GGA are modelled using the PBE functional [24]. This functional is known to accurately reproduce the ice-Ih ground-state properties, including hydrogen bonding [25]. The Kohn-Sham energies calculated for the 16-molecule supercell are shown in Fig. 1. Due to intermolecular interactions, the occupied molecular states $2a_1$, $1b_2$, $3a_1$, and $1b_1$ broaden into energy bands. We calculate a band gap of 5.6 eV, 0.6 eV smaller than the lowest molecular transition energy.

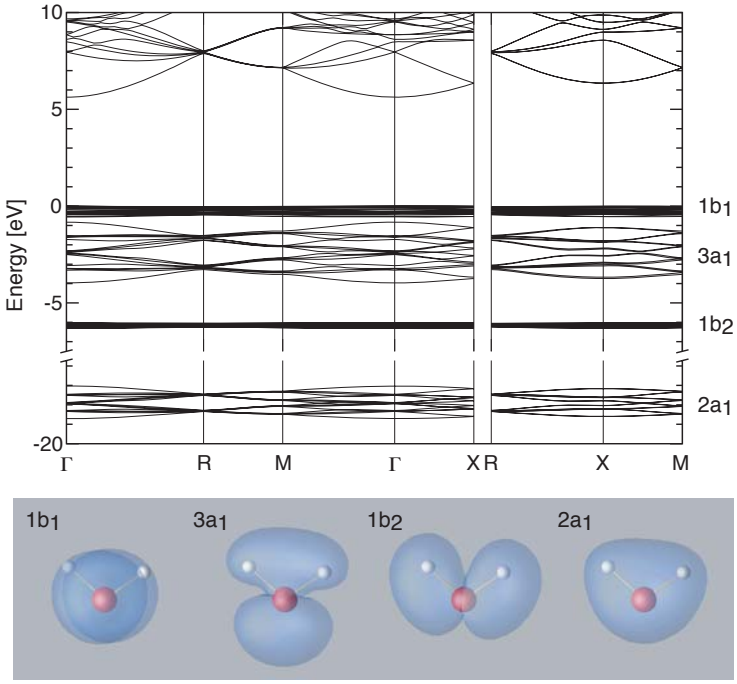

Fig. 1. Valence and conduction energy bands calculated in DFT-GGA for the 16 molecule supercell. The occupied molecular states, from which the valence bands are derived, are shown below.

Earlier DFT studies found an energy gap of about 6 eV for cubic ice [10] and 4.6 eV for the liquid [7].

The ground-state DFT calculations were parallelised for different bands and sampling points in the Brillouin zone using the message passing interface (MPI). Fig. 2 shows benchmark calculations to determine the electronic ground state of a water dimer starting from randomised wave functions. The calculations were performed on the Cray Opteron cluster of the Höchstleistungs-Rechenzentrum Stuttgart (2GHz AMD Opteron, Myrinet 2000 node-node interconnect), the Arminius cluster of the Paderborn Center for Parallel Computing (hpcline, Xeon EM64T 3.2 GHz, Infiniband) and a local Cray XD1 machine (2Ghz Dual Core AMD Opteron, RapidArray Interconnect). As can be seen, for systems of the size studied here, an efficient parallelisation is possible using up to 16 nodes. It is interesting to note that the details of the node-node interconnect seem to be of minor importance for the speedup, due to the limited need for data exchange between the nodes during the calculations.

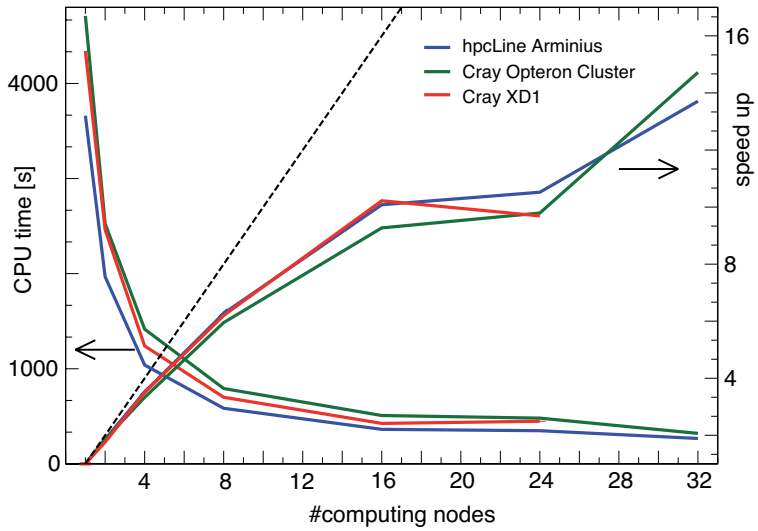

Fig. 2. CPU time per node and speed-up of a DFT-GGA ground-state calculation for the water dimer vs. number of nodes. The calculations were performed on the HLRS Opteron cluster, the PC^2 Xeon cluster and the Cray XD1 (see text).

In the second step we include electronic self-energy effects. This requires the replacement of the GGA exchange and correlation potential by the non-local and energy-dependent self-energy operator $\Sigma(\mathbf{r},\mathbf{r}';E)$. We calculate Σ in the GW approximation [15], where it is expressed as a convolution of the single-particle propagator G and the dynamically screened Coulomb interaction W. For single water monomers, the screening was obtained from *first principles*, using the random-phase approximation. Numerical details are given in [14]. For bulk water, a further approximation had to be introduced to cope with the numerical load: We use a model dielectric function [26] to calculate W. This speeds up the calculations substantially and results in quasiparticle energies that are within about 0.1 – 0.2 eV of the complete calculations [27, 28].

The electron-hole interaction is taken into account in the third step. The two-particle Hamiltonian

$$\begin{aligned} H_{vc\mathbf{k},v'c'\mathbf{k}'} &= (\epsilon_{c\mathbf{k}}-\epsilon_{v\mathbf{k}})\delta_{vv'}\delta_{cc'}\delta_{\mathbf{k},\mathbf{k}'}+ \\ &2\iint d\mathbf{r}d\mathbf{r}'\psi^*_{c\mathbf{k}}(\mathbf{r})\psi_{v\mathbf{k}}(\mathbf{r})\bar{v}(\mathbf{r}-\mathbf{r}')\psi_{c'\mathbf{k}'}(\mathbf{r}')\psi^*_{v'\mathbf{k}'}(\mathbf{r}') - \\ &\iint d\mathbf{x}d\mathbf{r}'\psi^*_{c\mathbf{k}}(\mathbf{r})\psi_{c'\mathbf{k}'}(\mathbf{r})W(\mathbf{r},\mathbf{r}')\psi_{v\mathbf{k}}(\mathbf{r}')\psi^*_{v'\mathbf{k}'}(\mathbf{r}') \ , \end{aligned} \tag{1}$$

describes the interaction of pairs of electrons in conduction states $|c\mathbf{k}\rangle$ and holes in valence states $|v\mathbf{k}\rangle$ [19, 20, 21]. The diagonal first part is given by the quasiparticle energies obtained in GW approximation. The second, the electron-hole exchange term, where the short-range part of the bare Coulomb potential $\bar{v}$ enters, reflects the influence of local fields. Finally, the third part, which describes the screened electron-hole attraction, is calculated using the same approximations for W as in the self-energy.

The eigenvalues and eigenvectors of the two-particle Hamiltonian (1) can be used to calculate the macroscopic dielectric function and thus the absorption spectrum. In the case of ice Ih, the Hamiltonian has been set up from 64 valence and 64 conduction bands using 40 $\mathbf{k}$ points. In order to bypass the diagonalisation of the Hamiltonian, we follow Glutsch *et al.* [29, 30]: If the energy dependence of the macroscopic polarisability on the eigenvalues of the exciton Hamiltonian is Fourier transformed, the polarisability can be obtained from the solution of an initial-value problem for the vector $|\mu(t)\rangle$. Its time evolution is driven by the pair Hamiltonian (1)

$$i\hbar|\dot{\mu}(t)\rangle = H|\mu(t)\rangle \ . \tag{2}$$

The initial values of the vector elements are given by

$$\mu^{i}_{cv\mathbf{k}}(0) = \frac{\langle c\mathbf{k}|v_i|v\mathbf{k}\rangle}{\epsilon^{LDA}_{c\mathbf{k}} - \epsilon^{LDA}_{v\mathbf{k}}} \ , \tag{3}$$

where v_i is the $i(= x, y, z)$ component of the velocity operator. The macroscopic dielectric function with the broadening parameter γ is then obtained by the Fourier transform of $e^{-\gamma t} \cdot \langle \mu(0)|\mu(t)\rangle$.

3 Results

The ice optical spectra calculated according to the three levels of theory described above are compared with experiment [2] in Fig. 3. The spectrum obtained within DFT-GGA agrees with earlier independent-particle results [10]. The calculated onset of absorption occurs at too low energies (below 6 eV), and the first absorption maximum at about 8 eV is far less pronounced than the corresponding feature in experiment. The inclusion of the many-body electron-electron interaction in GWA, *i.e.*, the electronic self-energy, leads to a nearly rigid blueshift of the spectrum, severely overestimating the energy positions of the measured peaks. The Coulomb correlation of electrons and holes, accounted for by solving the BSE, leads to the appearance of a sharp excitonic peak below the onset of the vertical quasiparticle transition energies. The peak positions and the line shape obtained from the BSE agree well with experiment. Since no input parameters to the calculation have been taken from experiment or fitted, the agreement between theory and measurement is truly impressive.

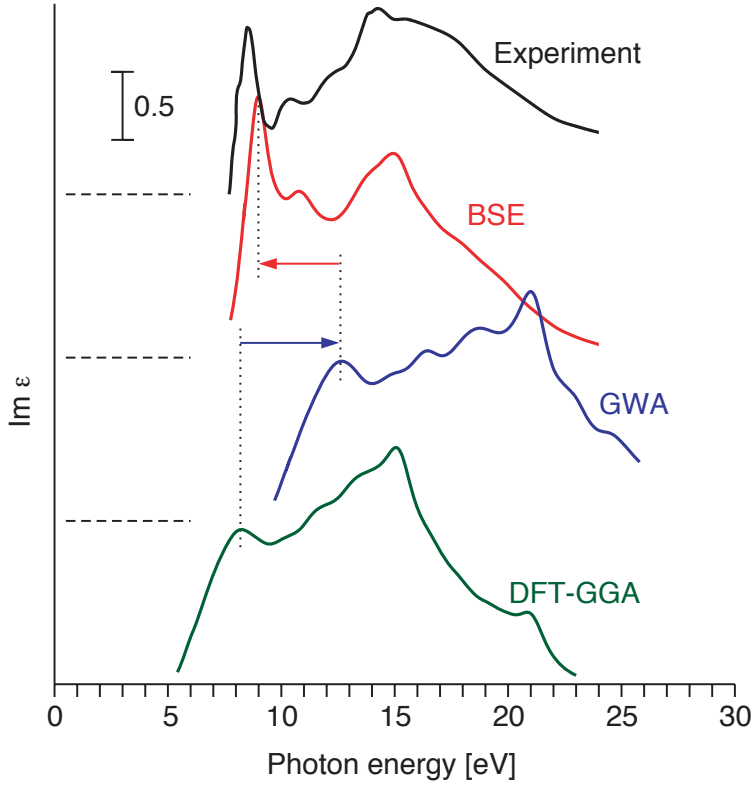

Fig. 3. Imaginary part of the dielectric function of hexagonal ice measured at 80 K (from Ref. [2]), and calculated within the DFT-GGA, the GWA, and from the BSE (see text).

After having reproduced the main features of the optical absorption of ice, we explore the origin of the prominent first peak. To this end we calculate the optical transitions of gas-phase H_2O molecules. The water monomer was modelled in a periodic (simple cubic) supercell with with a lattice constant of 10 Å. The DFT-GGA ground-state calculation yield a oxygen-hydrogen bond length of 0.966 Å and an angle between the two bonds of 104.49°. The corresponding experimental values for gas-phase molecules are 0.957 Å and 104.47°. According to the molecule symmetry, the atomic orbitals are derived from six linear combinations of a_1, a_2, b_1, and b_2 symmetry with non-degenerate energy levels. The eight valence electrons occupy the four lowest states. The dependence of the self-energy on the singe-particle eigenvalues is shown in Fig. 4. It is most important for the occupied molecular states, but nearly vanishes for the unoccupied states. The quasiparticle shifts vary between -7.7 and -4.7 eV (0.4 and 0.8 eV) for the occupied (empty) states.

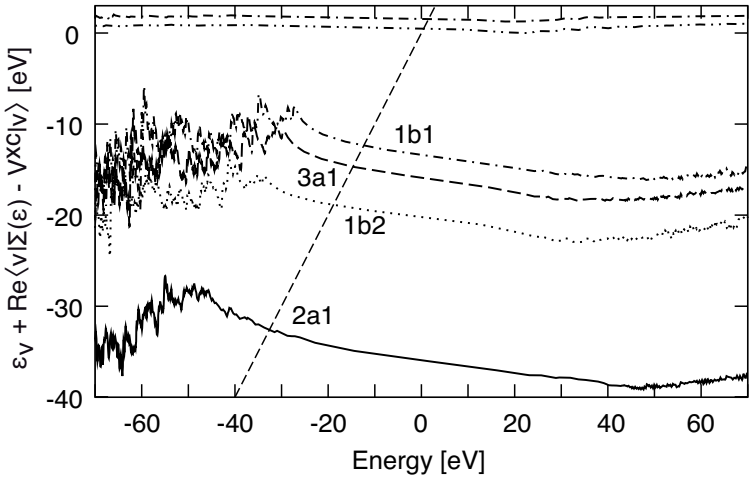

Fig. 4. Real part of the H_2O self-energy differences added to the corresponding KS eigenvalues versus single-particle excitation energy. The frequency-dependent dielectric matrix has been computed including 260 states. The straight short-dashed line represents the linear function ε. The crossings with the other lines define the quasiparticle energies $\varepsilon_\nu^{\mathrm{QP}}$.

At the single-particle level of theory, *i.e.*, in DFT-GGA, an energy of 6.2 eV is obtained for the lowest singlet pair excitation. The electronic self-energy blueshifts this value by 6.3 eV to 12.5 eV. This is partially compensated by an exciton binding energy of 5.3 eV, leading finally to an optical absorption at 7.2 eV, in excellent agreement with the experimental value of 7.4 eV [6].

These results can be compared with those for ice, shown in Fig. 3, where we find for the first absorption peak a self-energy shift of about 4.5 eV (blue arrow) and an exciton binding energy (related to the position of the first major peak of the vertical quasiparticle transitions, red arrow) of 3.2 eV. Self-energy and excitonic effects in ice are thus reduced by 29 and 40%, respectively, compared to gas-phase molecules. The reduction of the self-energy and the exciton binding energy upon condensation of the molecules is expected, due to the larger screening in the solid. The fact, however, that the exciton binding energy is affected more than the self-energy points to an additional effect, namely a change in the localisation of the exciton. The attractive interaction between an electron and a hole is inversely proportional to their average distance, the so-called exciton radius

$$R = \int d\mathbf{r}_e \int d\mathbf{r}_h |\mathbf{r}_e - \mathbf{r}_h| |\Psi(\mathbf{r}_e, \mathbf{r}_h)|^2, \tag{4}$$

where $\Psi(\mathbf{r}_e, \mathbf{r}_h)$ is the electron-hole pair wave function depending on the positions $\mathbf{r}_e$ and $\mathbf{r}_h$ of electrons and holes, respectively. The spatial distribution of electron-hole pairs therefore influences their energy.

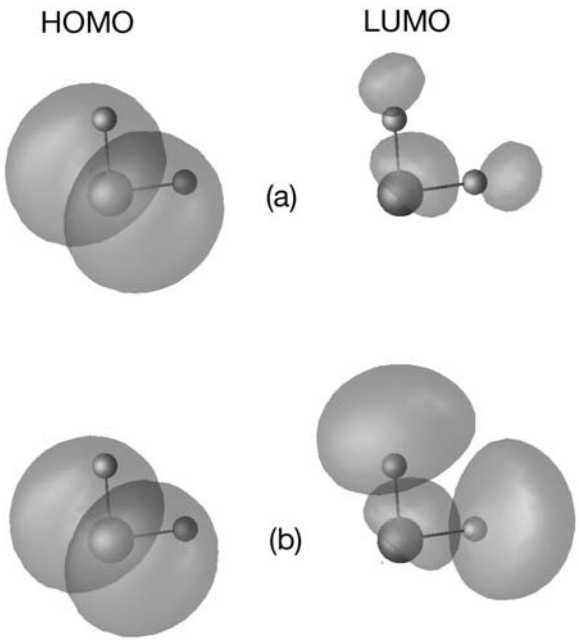

Fig. 5. HOMO and LUMO of the gas-phase water molecule in the ground state (a) and upon optical excitation (b).

In the case of an isolated molecule, the localisation of the electron-hole pair is immediately obtained from the spatial extension of the respective molecular orbitals, which relax upon optical excitation. The highest occupied molecular orbital (HOMO) of water is a nonbonding oxygen-localized $1b_1$ orbital. It barely changes upon excitation of one electron into the lowest unoccupied molecular orbital (LUMO). The latter, however, is strongly affected by partial occupation. The LUMO shows a significant probability density in the proximity of the O atom, as well as two lobes that protrude from the molecule in the proton directions, see Fig. 5(a). Optical excitation of one electron from the HOMO into the LUMO leads to a considerable expansion of these lobes, as shown in Fig. 5(b). Nevertheless, due to the attractive interaction with the hole at the oxygen atom, the electron remains close to the molecule. We calculate an average electron-hole distance R of 2.27 Å.

How does the spatial distribution of the excited electrons change upon condensation of the H_2O molecules? The solution of the BSE yields correlated electron-hole pair states. The pair wave functions $\Psi(\mathbf{r}_e, \mathbf{r}_h)$ are scalar

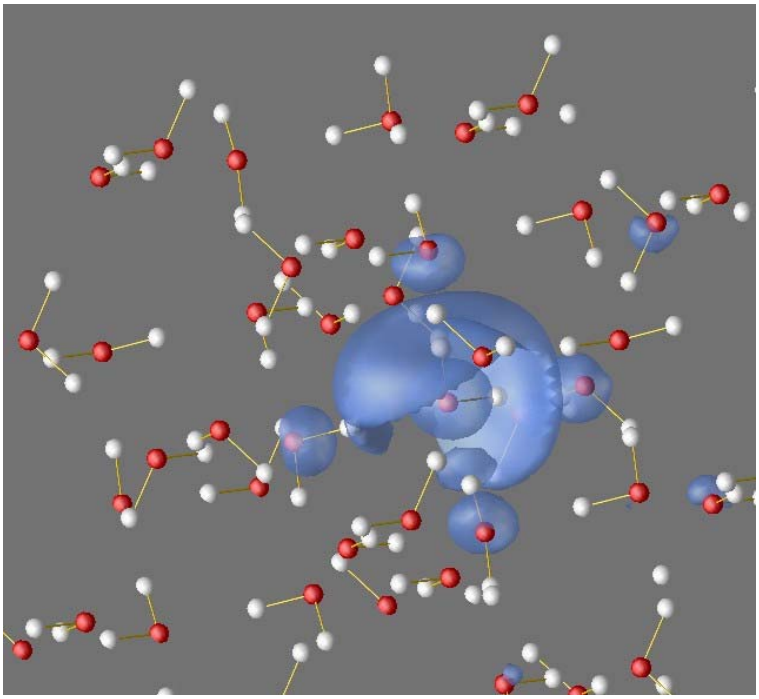

Fig. 6. Spatial distribution of the electron in the exciton associated with the lowest optical absorption peak of ice-Ih.

functions in the two-particle space. The center of gravity of the hole belonging to the exciton wave function responsible for the first absorption peak is close to an oxygen position τ_{oxygen}. In Fig. 6 we show the probability density $|\Psi(\mathbf{r}_e, \mathbf{r}_h = \tau_{oxygen})|^2$ corresponding to the electron distribution of that particular exciton. It is still reminiscent of the molecular LUMO shown in Fig. 5, but it expanded considerably farther towards the nearest-neighbour molecules. The calculated mean distance R between the electron and the hole is 4.02 Å, much larger than in the case of a gas-phase water molecule.

4 Conclusions

Our work shows that (i) the three-step approach consisting of DFT-GGA ground-state calculations, quasiparticle calculations within the GWA and the solution of the Bethe-Salpeter equation for the polarizability is appropriate to investigate excited-state properties of water structures. (ii) The water monomer exciton is extremely sensitive to hydrogen-bonded neighbour molecules. This suggests the possibility of detecting changes in the solvation

shell due to missing molecules or distorted hydrogen bonds by means of optical spectroscopy. The proposed calculations should thus be very helpful to clarify the interaction of water molecules with each other and also with foreign molecules. (iii) The simulations provide an intuitive explanation for the surprising energy shift discovered in experiments: The matrix of surrounding H_2O molecules enables the optically excited electron to move farther away from the hole left behind at the oxygen atom, thus reducing the binding energy of the electron-hole pair from 5.3 to 3.2 eV. This effect overcompensates the narrowing of the HOMO-LUMO energy gap resulting from the condensation of the H_2O molecules and leads to the observed blueshift of the optical absorption.

Generous grants of computer time from the Höchstleistungs-Rechenzentrum Stuttgart (HLRS) and the Paderborn Center for Parallel Computing (PC^2) are gratefully acknowledged.

References

1. R Onaka and T. Takahashi, J. Phys. Soc. Jpn. **24**, 548 (1968).
2. K Kobayashi, J. Phys. Chem. **87**, 4317 (1983).
3. G D Kerr, R N Hamm, M W Williams, R D Birkhoff, and L R Painter, Phys. Rev. A **5**, 2523 (1972).
4. H Hayashi, N Watanabe, Y Udagawa, and C-C Kao, Proc. Natl. Acad. Sci. USA **97**, 6264 (2000).
5. V F Petrenko and I A Ryzhkin, Phys. Rev. Lett. **71**, 2626 (1993).
6. W F Chan, G Cooper, and C E Brion, Chem. Phys. **178**, 387 (1993).
7. K Laasonen, M Sprik, M Parrinello, and R Car, J. Chem. Phys. **99**, 9080 (1993).
8. G P Parravicini and L Resca, Phys. Rev. B **8**, 3009 (1973).
9. L Resca and R Resta, phys. stat. sol. (b) **81**, 129 (1977).
10. W Y Ching, M-Z Huang, and Y-N Xu, Phys. Rev. Lett. **71**, 2840 (1993).
11. B D Bursulaya, J Jeon, C-N Yang, and H J Kim, J. Phys. Chem. A **104**, 45 (2000).
12. G Onida, L Reining, and A Rubio, Rev. Mod. Phys. **74**, 601 (2002).
13. P H Hahn, W G Schmidt, K Seino, M Preuss, F Bechstedt, and J Bernholc, Phys. Rev. Lett. **94**, 037404 (2005).
14. P H Hahn, W G Schmidt, and F Bechstedt, Phys. Rev. B **72**, 245425 (2005).
15. M S Hybertsen and S G Louie, Phys. Rev. B **34**, 5390 (1986).
16. S Albrecht, L Reining, R Del Sole, and G Onida, Phys. Rev. Lett. **80**, 4510 (1998).
17. L X Benedict, E L Shirley, and R B Bohn, Phys. Rev. Lett. **80**, 4514 (1998).
18. M Rohlfing and S G Louie, Phys. Rev. Lett. **83**, 856 (1999).
19. L J Sham and T M Rice, Phys. Rev. **144**, 708 (1966).
20. W Hanke and L J Sham, Phys. Rev. B **12**, 4501 (1975).
21. W Hanke and L J Sham, Phys. Rev. B **21**, 4656 (1980).
22. I Morrison, J-C Li, S Jenkins, S S Xantheas, and M C Payne, J. Phys. Chem. B **101**, 6146 (1997).
23. E L Briggs, D J Sullivan, and J Bernholc, Phys. Rev. B **54**, 14362 (1996).

24. J P Perdew, K Burke, and M Ernzerhof, Phys. Rev. Lett. **77**, 3865 (1996).
25. D R Hamann, Phys. Rev. B **55**, R10157 (1997).
26. F Bechstedt, R Del Sole, G Cappellini, and L Reining, Solid State Commun. **84**, 765 (1992).
27. J E Northrup, Phys. Rev. B **47**, R10032 (1993).
28. W G Schmidt, S Glutsch, P H Hahn, and F Bechstedt, Phys. Rev. B **67**, 085307 (2003).
29. S Glutsch, D S Chemla, and F Bechstedt, Phys. Rev. B **54**, 11592 (1996).
30. P H Hahn, W G Schmidt, and F Bechstedt, Phys. Rev. Lett. **88**, 016402 (2002).